

HYDRODYNAMIC ASPECTS OF FLUIDIZED BED STABILIZED IN MAGNETIC FIELD

Alina-Violeta URSU¹, Ileana Denisa NISTOR², Fabrice GROS³, Alisa Vasilica ARUŞ⁴, Gabriela ISOPENCU⁵, Alina Monica MAREŞ⁶

Lucrarea își propune studiul hidrodinamic al particulelor feromagnetice (oțel comercial) în cazul fluidizării gaz/solid în câmp magnetic. S-a studiat influența caracteristicilor particulelor solide (magnetice), intensității câmpului magnetic (în domeniul 0-12000 A. m-1), asupra căderii de presiune și porozității stratului granular. Rezultatele arată faptul că intensitatea câmpului magnetic are o importanță mare asupra stabilității particulelor magnetice în strat monocomponent.

The paper studies the hydrodynamic of the gas/solid fluidization in a transverse magnetic field of ferromagnetic particles (commercial steel). The influence of solid (magnetic and non-magnetic particles) characteristics, and the magnetic field intensity (in the range of 0-12000 A.m-1), on the pressure drop and porosity of the granulated bed has been investigated. The results confirm that the magnetic field intensity has a large influence on the stability of magnetic particles in a mono-component bed.

Keywords: hydrodynamic of magnetic particles, magnetic field intensity

1. Introduction

Magnetically stabilized fluidized beds (MSFB) represent a new technology for eliminating the drawbacks of the classical fluidized beds [1]. Fluidization in (electro) magnetical field combines the desirable characteristics of the both fluidized and packed bed, i.e. a low pressure drop of fluidized bed, with the bubble free operation at high gas velocity of packed bed [2], with the immediate result of an improved G-S contact efficiency. MSFB is a widespread technique of variate applications in combustion of solid fossil fuels [3], methane-carbon dioxide catalytic reforming [4], and separation processes, such as the magnetic-

¹ Lecturer, University “Vasile Alecsandri” of Bacau, 157 Calea Marasesti, RO-600115, Romania, e-mail: alina_violeta_ursu@yahoo.com

² Professor, University “Vasile Alecsandri” of Bacau, 157 Calea Marasesti, RO-600115, Romania

³ Lecturer, Clermont Université, ENSCCF, LGCB, BP 10448, F-63000 Clermont-Ferrand, France

⁴ Assistant, University “Vasile Alecsandri” of Bacau, 157 Calea Marasesti, RO-600115, Romania

⁵ Lecturer, Faculty of Applied Chemistry and Materials Science, University POLITEHNICA of Bucharest, Romania

⁶ Engineer, Faculty of Applied Chemistry and Materials Science, University POLITEHNICA of Bucharest, Romania

nonmagnetic dust-filtration, ion exchange, adsorption [5], copper cementation [6-7], yeast filtration [8], particle separation by density and magnetic properties [9-10], gas separation [5], ethanol fermentation [11], etc. The properties of MSFB make possible intensification of the mass transfer in gas-solid systems, of high importance in adsorption processes [5].

Utilization of natural adsorbents, of alumino-silicates type, in de-pollution processes has already been investigated [12, 13].

This paper presents a first stage of the MSFB method implementation for adsorption using clay adsorbents. Hence, the hydrodynamic study of the bed is necessary as well for determining the technological boundary values of some operating parameters, and to modulate the hydrodynamic properties of the solid particles.

The dynamic processing through fluidization implies the presence of some inter-particular forces [14], due to the small dimensions of the particles. To compensate these inter-particular forces, the use the magnetic field will be investigated. It is also necessary to determine the most important parameters of the granulated fluidised media in MSFB, with major importance in adsorption process.

2. Materials and methods

All the experiments have been carried out in a cylindrical glass column (Fig. 1), with a 0.5 m height and a 50 mm inner diameter. The gas distributor (and media bearer) consists in a P2 porous glass plate, whose pressure drop is high enough (3600 Pa at $0.34 \text{ m}\cdot\text{s}^{-1}$), for the investigated gas velocity range, to ensure a uniform gas admission in the porous media. Dry compressed air was used as fluidizing fluid, of inlet flowrate regulated by Brooks (GT 1024 and Shorate 1355) flowmeters. The schema of the experimental bench-scale plant is presented in Fig. 1. Pressure drops across the bed have been measured with a digital manometer Keller PD 33H (connected to wall pressure taps), linked to a computer via a Keller K-107 transducer. The porous media (bed) consists in steel shots (trade name WS70 or WS170 provided by Wheelabrator (Allevard, France)), and classified according to their diameters. Their physical properties (granulometric class, determined via sieving, density) are presented in Table 1.

The initial bed porosity is calculated with equation (1):

$$\varepsilon_0 = 1 - \frac{M_s}{\rho_s A L_0} \quad (1)$$

where M_s is the mass of solid contained in the bed, A the column section, and L_0 the bed initial height.

The transverse electromagnetic field is generated by a saddle coil device, designed following indications from literature [15-17]. The device consists in two

half cylindrical parts (made of PVC tube, 80 mm inner diameter), on which 0.8 mm diameter copper wire is winded up to get a saddle coil configuration generating the transverse field.

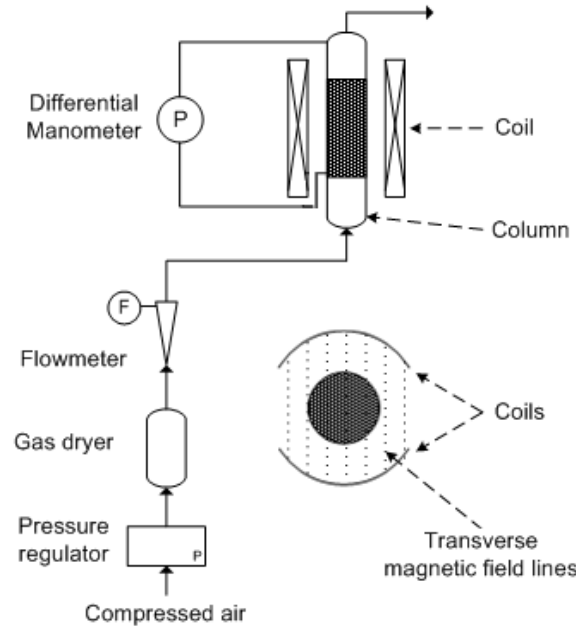


Fig. 1. Scheme of the hydrodynamic experimental bench-scale plant

Table 1

Physical properties of the particles

| Particle type | Composition | $d_p (10^{-3} m)$ | $\varepsilon_0 (-)$ | $\rho_s (kg.m^{-3})$ |
|---------------|--------------------|-------------------|---------------------|----------------------|
| WS 170 | Steel (Fe > 98.5%) | 0.5-1 | 0.44-0.45 | 7450 |
| | | 0.2-0.5 | 0.43-0.44 | 7450 |

The electrical power is supplied and controlled by a Lambda generator (model FV 345, in the range 0-5 A) to get a chosen value of the electromagnetic field intensity (H). This parameter was measured with a Magnet-Physik FH 51 gaussmeter, equipped with a HS-TB51 transverse probe, being function of spatial position and current intensity (I). The magnetic field homogeneity is all-times checked in the region of interest (the porous media), field intensity deviation being less than 3%, at distances between 10 and 35 cm from source.

For instance, Fig. 2 presents the transverse field intensity distribution in the centre of the cross section for various electrical power intensities, and at various vertical positions (the origin being on top of the coils). As expected, the field intensity varies linearity with the juice intensity.

The horizontal plane component of the magnetic field vector was also evaluated, being proved as being negligible (less than 1/16 of the transverse field intensity).

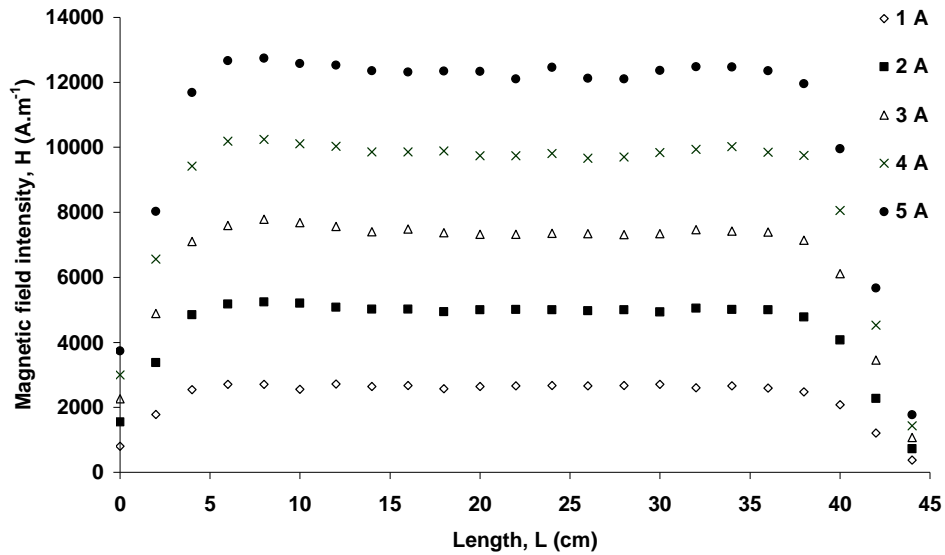


Fig. 2. Field intensity profile according to current intensity and position

All experiments were carried out in solid batch/field FIRST mode, as was proposed and denominated by Siegell [18], and generalised by Hristov [19]. A certain amount of solid was first introduced in the reactor (solid batch), being fluidized and gently defluidized (giving a L_0 high bed) to get reproducible initial bed states. Various initial bed heights have been used, from 5 cm up to 20 cm. The electrical power (and so the electromagnetic field) is turned on. Gas is then allowed to flow through the bottom inlet of the column.

3. Results and discussions

3.1. Hydrodynamic behaviour of the ferromagnetic particles in the fluidized bed

Experiments conducted in the absence of the magnetic field ($H=0$) exhibits a classical pressure drop behaviour. Fig. 3 plots indicate an increase of the pressure drop across the packed bed, of a curve shape in accordance to an Ergun-type relation, with a linear predominant term (Reynolds number being close to unity) for WS 70 (a), and a more sensible slope change for WS 170 (b) particle (intermediary flow regime), until the minimum fluidization velocity is reached (Table 2). Experimental values are in good agreement with those, predicted by the

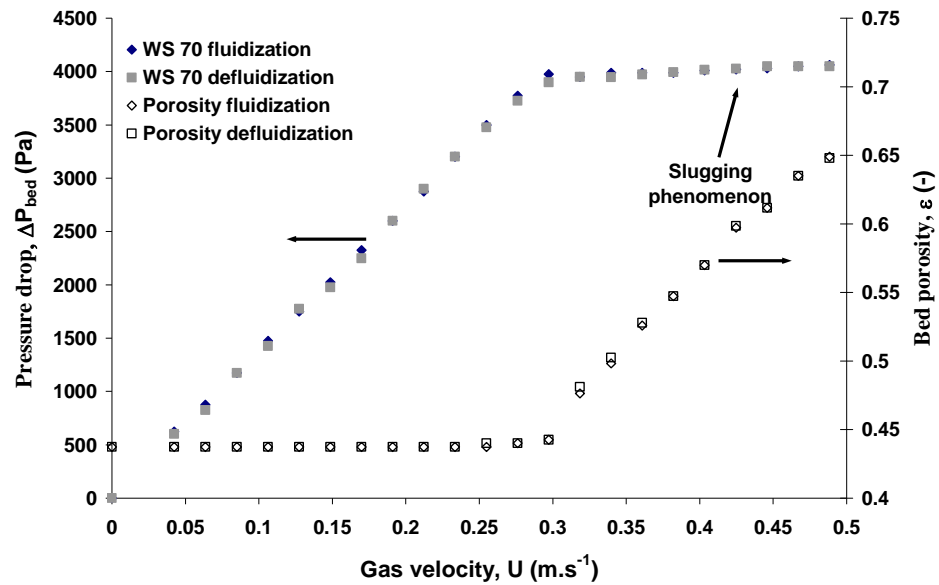
Lucas et al. [20] correlation for round particles of WS 70 and WS 170. Beyond U_{mf} , the bed is expanded and fluidized.

Table 2

Experimental and calculated values for minimum fluidization velocity

| Experimental U_{mf} (m.s ⁻¹) | Calculated U_{mf} (m.s ⁻¹) |
|--|--|
| 0.76 | 0.74 |
| 0.3 | 0.29 |

The experimental pressure drop is constant (roughly 4000 Pa) being close to the theoretical value of weight per unit of area of the bed, the small deviation being explained by the pressure tap position.



a)
Fig. 3.a) Hydrodynamic behaviour of WS 70

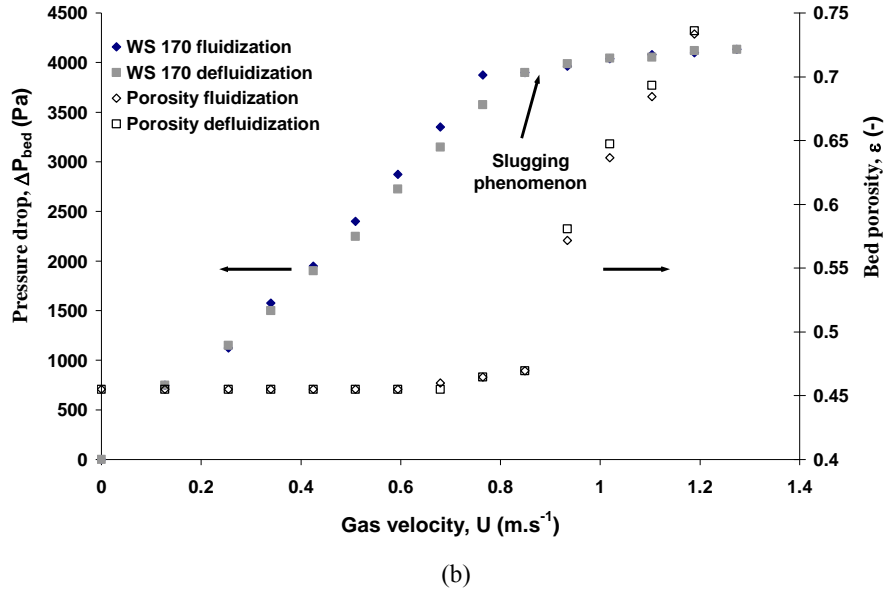


Fig. 3.b) Hydrodynamic behaviour of WS 170

Although the bed height is small ($L_0=10$ cm), wall or B type slugs appear (according to the classification of Yang [22]). This slug development has been attributed to the pressure tap, that generates an irregularity over the column cross section. Moreover, its appearance seems to not depend on the particle diameter, the slugging mode being reached for both cases at a gas velocity of 0.1 m.s⁻¹ higher than $U_{mf, H=0}$, even if a difference according to the Geldart's classification still exists [22]: regime B for WS70 (corresponding to a sand like behaviour), and regime D for WS170 (corresponding to a spoutable particle bed).

One can remark that the pressure drop increases linearly with the gas flowrate (above the theoretical apparent weight per square unit) (Fig. 3). This observation is in agreement with those derived by *Chen et al.* [23], and can be explained by either the energy necessary to continuously accelerate the solids, or by the potential energy dissipated by the solids [24].

The bed surface (and thus the pressure drop) of the slugging bed alternatively oscillates between a maximum and a minimum position, following the eruption of the slug [22]. The average bed porosity is represented in the Fig. 3. As expected, the slug frequency (hence the pressure drop oscillation) appears to be independent of the gas velocity, over the investigated operating small range [25].

3.2. Hydrodynamic behaviour of a ferromagnetic particle bed under magnetic field

3.2.1. Pressure drop

As noticed before [26, 27], for gas velocities lower than the minimum fluidization velocity, and for identical initial bed states, the pressure drop is not modified by the presence or absence of the magnetic field.

Beyond $U_{mf, H=0}$, the pressure drop slope is slightly modified by the magnetic field intensity (Fig. 4). In a gas/solid fluidization under magnetic field, depending on field intensity two characteristic velocities can be pointed out [26]:

- the bed expansion velocity U_e , where the upper layer of the bed begins to expand;
- the bubbling velocity, U_b .

In this study, U_b is considered a slug formation, corresponding to the homogeneous bed structure partial destruction. For such a velocity, the magnetic interactions are not strong enough compared to the drag forces to maintain a stable bed and to avoid slug formation. Between those two velocities, the bed is magnetically stabilized and expanded.

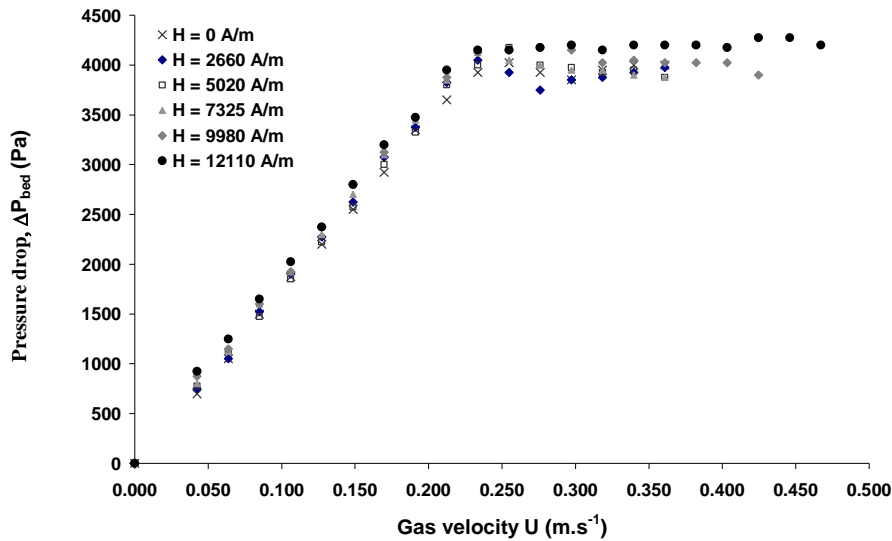


Fig. 4. Variation of pressure drop with gas velocity for different magnetic fields

To have a better understanding of bed behaviour, state diagram can be plotted showing the evolution of U_e and U_b , as function of field intensity (see Fig. 5). These graphs visualise the conditions under which the bed is fixed ($U_0 < U_e$),

magnetically fluidized and stabilized ($U_e < U_0 < U_{mf, H}$), or partially stabilized with slugs ($U_0 > U_{b, H}$). The graphs can be used to predict the bed behaviour according to the used operating parameters.

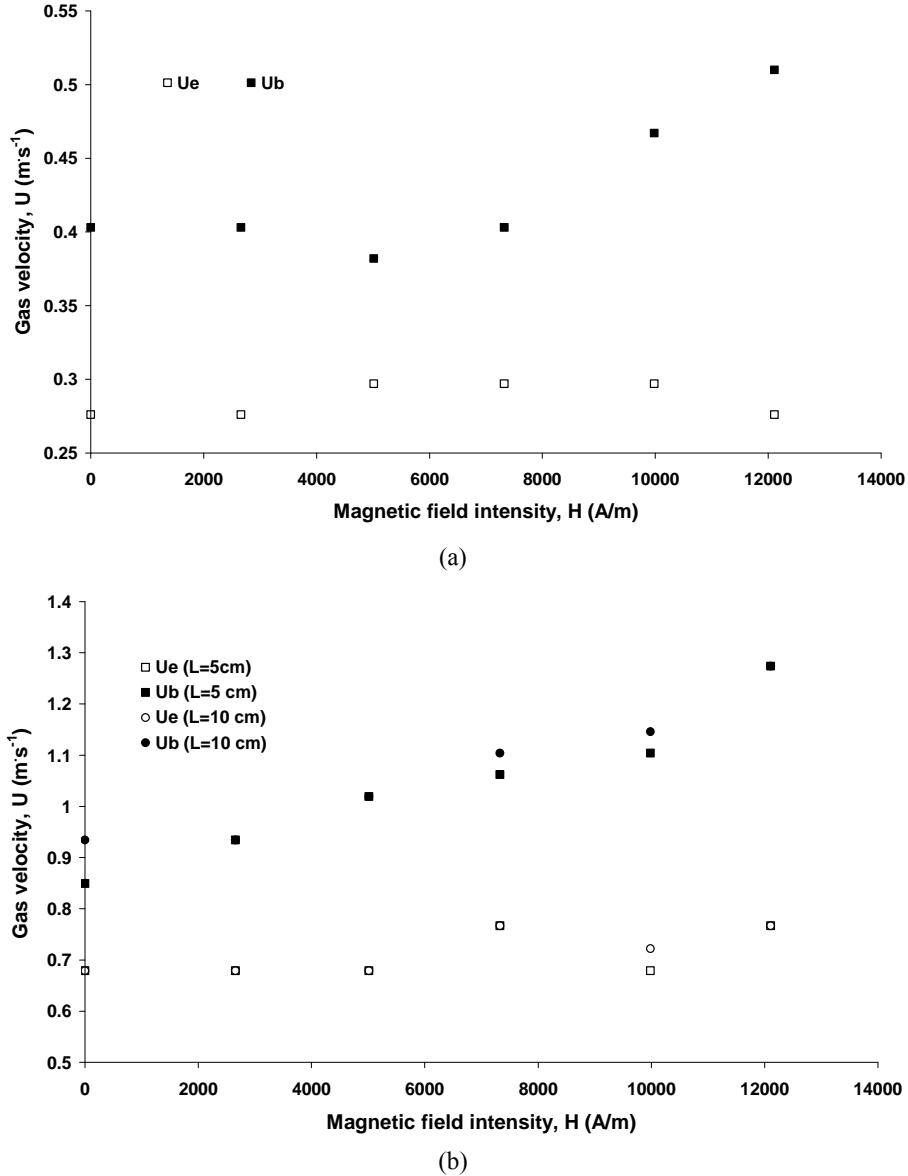


Fig. 5. State diagrams for WS 70 (a) and WS 170 (b)

Following the experimental results, the minimum velocity of bed expansion U_e is nearly constant (for WS 70), or it slightly increases with the magnetic field intensity. On the other hand, $U_{b,H}$ increases with the intensity of the magnetic field. Linear relationships [26-27], or of exponential form [19] can be used to describe the evolution of these two velocities:

$$U_e = U_{mf, H=0} + k_e H \quad (2)$$

$$U_{b,H} = U_{mf, H=0} + k_{max} H \quad (3)$$

Table 3

| Values of k_e and k_{max} coefficients | | |
|--|-----------------------------------|---------------------------------------|
| Trade name | $k_e (10^{-6} m^2 s^{-1} A^{-1})$ | $k_{max} (10^{-5} m^2 s^{-1} A^{-1})$ |
| WS70 | Not significant | 2.2 (for the three last points) |
| WS170 | 7 | 3.0 |

The low values of k_e and k_{max} recommend the use of the linear model, and not of the exponential model.

In transverse field gas/solid fluidization [19] (and opposite to of axial field results), the velocity U_e increases with field intensity, due to the attraction forces among the particles. The relative weak intensity of our magnetic field can explain the relative independency of U_e in our case.

According to Thivel et al [27], the factor k_{max} represents the cohesion within the bed created by the magnetic field leading to a delay in slug outbreak. The values presented in table 3 are of the same order of magnitude as those observed by several authors [26-27].

Excess of pressure drop, typical from fluidization under transverse magnetic field [7, 27], could not have been clearly identified under the investigated operating conditions, the magnetic field being as weak as those recorded when the water is used as a fluidizing agent [20]. However, our results are in agreement with those of Hristov [29], where pressure in stabilized and the transverse and axial operating modes are similar (?).

3.2.3. Porosity evolutions

Bed porosity could be another pertinent parameter to describe the behaviour of our system. The bed porosity ε is calculated from the mass balance, by taking into account L , L_0 and ε_0 :

$$\varepsilon = 1 - \frac{L_0}{L} (1 - \varepsilon_0) \quad (4)$$

The experimental values of the initial porosity presented in Table 1 are in good agreement with the reported values obtained for spherical particles [30]. The

evolution of the porosity according to H and U_0 (Fig. 6) confirms the results presented in Fig. 5: the bed expands at nearly constant velocity U_e although higher magnetic field intensities have been applied. For identical velocity regime in the MSFB, the bed display a porosity as lower as the field intensity increases.

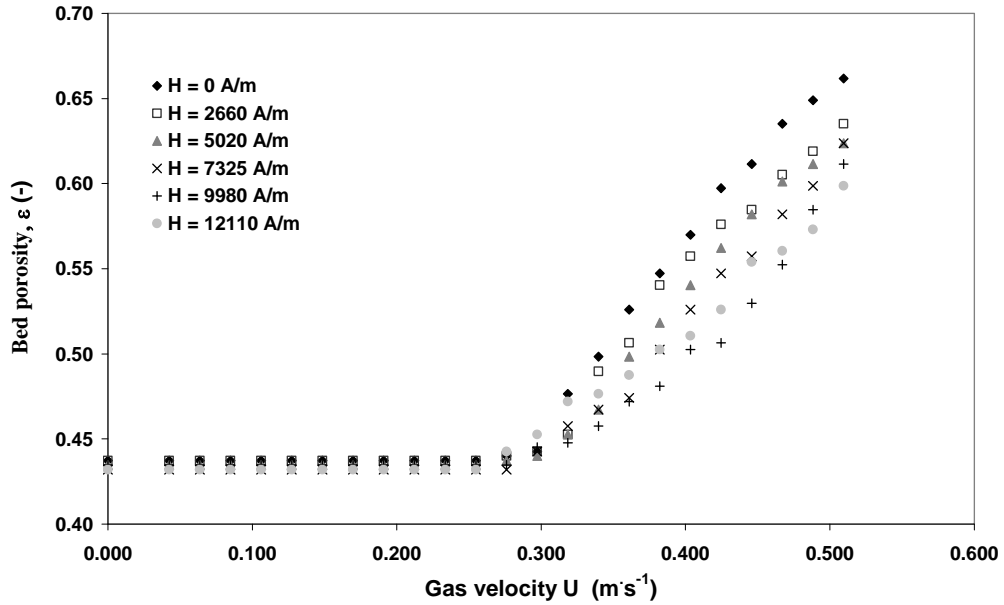


Fig. 6. Porosity evolution according to gas velocity and magnetic field intensity

This bed contraction has been previously attributed to the magnetic system size limitation if compared to the bed height [7], and both for the liquid/solid fluidization cases. Such porosity evolution results are opposite to the observations of Penchev et al. [31], where size limitation of the generated field appeared to be absent. Such a difference can be explained by the reduction or suppression of the local void porosities, and by the physical properties of the used particles. However, further investigations should be carried out by using other type of particles in the same magnetic field.

3.2.4. Hysteresis phenomena during cycling

It is known that during a fluidization–defluidization cycle, the pressure drop through the bed and its porosity are roughly the same at increasing or decreasing fluid flowrates. In our study, the fluidization–defluidization cycles were carried out under electromagnetic field, a set of typical result being presented in Fig. 7, where the hysteresis loops can be clearly identified.

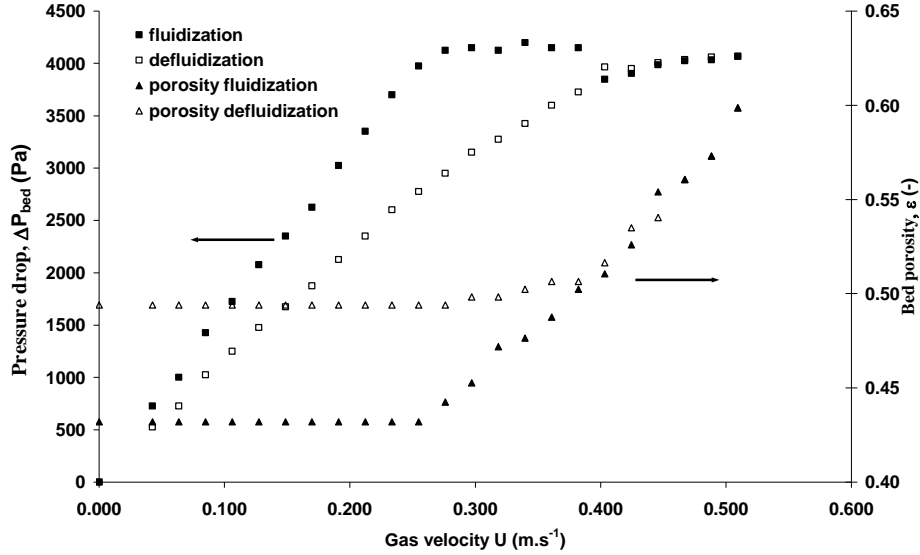


Fig.

7: Pressure drop porosity evolution hysteresis according to gas velocity during fluidization and defluidization cycle (WS 70, $L_0 = 10$ cm, $H = 12110$ A.m $^{-1}$)

When the gas velocity is increased, once the MSFB regime is passed, slugging phenomena occurs. Then, for decreasing flowrates, the homogeneous MSFB state cannot be obtained, due to the electromagnetic forces, and the bed keeps its heterogeneous channelling structure, or with local voids, as mentioned by Hristov for transverse fields [19]. Consequently, the gas flows easily and the pressure drop decreases regularly, leading to values lower than those indicated by a classical fluidization. Additionally, the cyclic fluidization-defluidization operations of magnetically stabilized bed display higher porosities of the final bed, due to the existence of the remaining slits.

6. Conclusions

Fluidization experiments were carried out using ferromagnetic particles. Monocomponent beds exhibited a classical behaviour, that is a filtration and fluidization regime, a minimum fluidization velocity in agreement with the literature correlations. At higher air velocities in a fluidization mode, slugging phenomenon, subsequent pressure drop and bed height oscillations occurred for ferromagnetic particles.

Under a transverse magnetic field, the slug outbreak was postponed (using various flowrates), and the outbreak intensity (monitored by pressure drop standard deviation) was also reduced. The predictive tools of the fluidised bed

behaviour, such as the phase diagrams (exhibiting fixed, stabilized and slugging bed regimes) can be thus useful for further plant design and operation.

Symbol

| | |
|-----------------|--|
| A | Cross-section of the column (m^2) |
| d_p | Particle diameter or granulometric class (m) |
| H | Magnetic field intensity ($A m^{-1}$) |
| k_e | Expansion constant ($m^2 s^{-1} A^{-1}$) |
| k_{max} | Maximum stabilization constant ($m^2 s^{-1} A^{-1}$) |
| L_0 | Initial bed height (cm) |
| L | Bed height (cm) |
| M_s | Solid mass (kg) |
| U_0 | Superficial gas velocity ($m s^{-1}$) |
| U_b | Gas velocity at the appearance of gas bubbles or slugs ($m s^{-1}$) |
| U_e | Expansion velocity ($m s^{-1}$) |
| U_{mf} | Minimum fluidization velocity for $H=0$ ($m s^{-1}$) |
| $U_{mf, H}$ | Minimum fluidization velocity in the presence of magnetic field ($m s^{-1}$) |
| ΔP | Bed pressure drop (Pa) |
| ε | Bed porosity (-) |
| ε_0 | Initial bed porosity (-) |
| ρ_s | Material density ($kg m^{-3}$) |

R E F E R E N C E S

- [1] *M. V. Filipov*, The effect of a magnetic field on a ferromagnetic particle suspension bed, *Prik. Magnit. Lat. SSR*, 12, 1960, p. 215-220
- [2] *Y. A. Liu, R. K. Hamby, R. D. Colberg*, Fundamental and practical developments of magnetofluidized beds : a review, *Powder Technol.*, 64, 1991, p. 3-11
- [3] *Z. Al-Qodah, M. Al-Busoul, A. Khraewish*, Hydrothermal Behavior of G-S Magnetically Stabilized Beds Consisting of Magnetic and Non-Magnetic Admixtures, *ICCE 2007 – 4th International Conference on Chemical Engineering*, Berlin, Germany, 24-26 August 2007
- [4] *H. Zhigang, Z. Quingshang, J. Zheng, L. Hongzhong*, Fluidization characteristics of aerogel Co/Al₂O₃ catalyst in a magnetic fluidized bed and its application to CH₄-CO₂ reforming, *Powder Technology*, 183, nr 1, 2008, p. 46-52
- [5] *J. Hristov, K. Boyadzhiev, L. Pantoscheva*, Sulfur dioxide adsorption in a magnetically stabilized synthetic-anionite bed, *Theoretical Foundations of Chemical Engineering*, 34, nr 5, 2000, p. 439-443
- [6] *F. Gros, S. Baup, M. Aurousseau*, Intensified recovery of copper in solution: Cementation onto iron in fixed or fluidized bed under electromagnetic field, *Chemical Engineering and Processing: Process Intensification.*, 47, nr 3, 2008, p. 295-302
- [7] *F. Gros, S. Baup, M. Aurousseau*, Hydrodynamic study of a liquid/solid fluidized bed under transverse electromagnetic field, *Powder Technology*, 183, nr 2, 2008, p 152-160
- [8] *J. Hristov, L. Fachikov*, An overview of separation by magnetically stabilized beds: State-of-the-art and potential applications, *China Particuology*, 5, nr 1-2, 2007, p. 11-18

- [9] *M. Fan, Q. Chen, Y. Zhao, Z. Luo, Y. Guan, B. Li*, Magnetically stabilized fluidized beds for fine coal separation , Powder Technology, 123, nr 2-3, 2002, p.208-211
- [10] *V.I. Sikavitsas, R.T. Yang, M.A. Burns, Langenmayr E.J.*, Industrial & Engineering Chemical Research, 34, nr 8, 1995, p. 2873-2880
- [11] *C.-Z. Liu, F. Wang, F. Ou-Yang*, Ethanol fermentation in a magnetically fluidized bed reactor with immobilized *Saccharomyces cerevisiae* in magnetic particles, Bioresourche Technology, 100, nr 2, 2009, p.878-882
- [12]. *M. Vaduva, V. Stanciu*, Selective carbon dioxide adsorption from N2-CH4-CO2 mixture on carbon molecular sieves, U.P.B. Sci. Bull., Series B, Vol. 69, No. 4, 2007, p. 59-70
- [13]. *M. Ulmanu, I. Anger, E. Gament, G. Olanescu, C. Predescu, M. Sohaciu* Effect of a romanian zeolite on heavy metals transfer from polluted soil to corn, mustard and oat, U.P.B. Sci. Bull., Series B, **Vol. 68**, No. 3, 2006, p. 67-76
- [14]. *G. Isopencu, M. Mares, G. Jinescu*, Interparticular forces in powdery materials beds, U.P.B. Sci. Bull., Series B, **Vol. 69**, No. 3, 2007, p. 27-34
- [15] *C.E.G. Salmon, E. L. Gea Vidoto, M. J. Martins, A. Annus*, Optimization of saddle coils for magnetic resonance imaging, Brazilian Journal of Physics, 36, nr. 1A, 2006, p 4-8
- [16] *H. Hanssum*, Magnetic field of saddle-shaped coils: II. Transverse Components, Journal of Physics D: Applied Physics, 18, 1985, p. 1971-1978
- [17] *H. Hanssum*, The magnetic field of saddle-shaped coils: I. Symmetry of the magnetic field around the coil centre, Journal of Physics D: Applied Physics, 17, 1984, p. 1-18
- [18] *J.H. Siegell*, Magnetically frozen beds, Powder Technology, 55, nr. 2, 1988, p. 127-132
- [19] *J. Hristov*, Magnetic field assisted fluidization : a unified approach. Part 1. Fundamentals and relevant hydrodynamics of gas-fluidized beds (batch solids mode), Reviews in Chemical Engineering, 18(4-5), 2002, p. 295-509
- [20] *A. Lucas, J. Arnaldos, J. Casal, L. Puigjaner*, Improved equation for the calculation of minimum fluidization velocity, *Industrial and Engineering Chemistry Process Design and Development*, 25, 1986, 426-429.
- [21] *C. Wen, Y. H. Yu*, Mechanics of fluidization, Chemical Engineering Progress Symposium Series, 62, nr. 62, 1966, p. 100-111
- [22] *W.-C. Yang*, Bubbling fluidized bed, Handbook of fluidization and fluid particle systems, p 53-111
- [23] *Z.Chen, L. Gibilaro, Foscolo G.*, Fluid pressure loss in slugging fluidised beds, Chemical Engineering Science, 52, nr 1, 1997, p. 55-62
- [24] *R. Di Felice*, Liquid fluidised beds in slugging mode: pressure drop and flow regime transition, Powder Technology, 123, nr 2-3, 2002, p. 254-261
- [25] *C.R. Muller, J.F. Davidson, J.S. Dennis, P.S. Fennell, L.F. Gladden, A.N. Hayhurst, M.D. Mantle, A.C. Rees, A.J. Sederman*, Oscillations in gas-fluidized beds: Ultra-fast magnetic resonance imaging and pressure sensor measurements, Powder Technology, 177, nr 2, 2007, p. 87-98
- [26] *P. Contal*, Approche de la filtration des gaz par lit fluidisé stabilisé magnétiquement, Thesis of the Savoie University, Chambéry, France, 1994
- [27] *P.X. Thivel, Y. Gonthier, P. Boldo, A. Bernis.*, Magnetically stabilized fluidization of a mixture of magnetic and non-magnetic particles in a transverse magnetic field, Powder Technology, 139, nr 3, 2004, p. 252-257
- [28] *J. Y. Hristov*, Fluidization of ferromagnetic particles in a magnetic field Part 1: The effect of field line orientation on bed stability, Powder Technology, 87, nr 1, 1996, p. 59-66
- [29] *N. Ouchiyama, T.Tanaka*, Porosity estimation for random packings of spherical particles, Industrial and Engineering Chemistry Fundamentals, 23, 1984, p. 490-493

- [30] *I.P. Penchev, Z. Al-Hassan, J. Hristov*, La Fluidisation, Proceedings of the 6^{èmes} Journées Européennes sur la Fluidisation, Toulouse, 29–31 Janvier 1991, Récents Progrès en Génie des Procédés, Toulouse, 5, nr 11, 1991, p. 341–351
- [31] *S. Chiba, A. W. Nienow, T. Chiba, H. Kobayashi*, Fluidised binary mixtures in which the denser component may be flotsam, Powder Technology, 26, nr 1, 1980, p. 1-10.